GEOPHYSICS

Determination of intrinsic attenuation in the oceanic lithosphere-asthenosphere system

Nozomu Takeuchi,[1]* Hitoshi Kawakatsu,[1] Hajime Shiobara,[1] Takehi Isse,[1] Hiroko Sugioka,[2] Aki Ito,[3] Hisashi Utada[1]

We recorded *P* and *S* waves traveling through the oceanic lithosphere-asthenosphere system (LAS) using broadband ocean-bottom seismometers in the northwest Pacific, and we quantitatively separated the intrinsic (anelastic) and extrinsic (scattering) attenuation effects on seismic wave propagation to directly infer the thermomechanical properties of the oceanic LAS. The strong intrinsic attenuation in the asthenosphere obtained at higher frequency (~3 hertz) is comparable to that constrained at lower frequency (~100 seconds) by surface waves and suggests frequency-independent anelasticity, whereas the intrinsic attenuation in the lithosphere is frequency dependent. This difference in frequency dependence indicates that the strong and broad peak dissipation recently observed in the laboratory exists only in the asthenosphere and provides new insight into what distinguishes the asthenosphere from the lithosphere.

Plate tectonics is a unified framework that explains various phenomena on the surface of Earth; however, the physical mechanisms underlying plate tectonics are poorly understood. There is no consensus even on why the lithosphere (plates) and asthenosphere have different viscosities, and various efforts are being devoted to revealing their physical properties (*1*–*5*). Because the lithosphere-asthenosphere system (LAS) should be in its simplest form beneath the ocean, the characterization of its physical properties there is essential. Direct observation of the viscosity of the oceanic LAS is not currently feasible. Among various observable physical parameters, the frequency dependence of anelasticity is one of the most important, as anelasticity and viscosity are related through microphysics at the grain boundary of the mantle material. Although recent advances in broadband ocean-bottom seismology have confirmed the basic high-velocity lid and low-velocity zone (LVZ) structures (including anisotropy) (*6*–*8*) often associated with the lithosphere and asthenosphere, the anelastic structure remains poorly understood (*9*). Recent laboratory studies have begun to elucidate the wide spectrum of anelastic behavior in Earth's mantle, indicating that the frequency dependence of anelasticity is represented by peak dissipation superimposed on background dissipation (*10*, *11*), although the conditions and/or mechanisms that define the shape and location of dissipation peaks are still under debate (*11*, *12*). The ability to confirm and characterize such peaks in the oceanic LAS would allow us to infer the thermomechanical conditions responsible for the viscosity contrast that separates the lithosphere and asthenosphere.

The observational challenge for unraveling the anelastic structure originates in the difficulty of separating intrinsic (anelastic) and extrinsic (scattering, heterogeneity) attenuation effects in seismic records. Although broadband seismometers record waveforms over a wide frequency range (e.g., ~1000 s to 10 Hz), seismological analysis of anelasticity is limited to a narrow frequency band (*13*). For lower-frequency waves (<~0.02 Hz), we can correct for the effects of extrinsic attenuation, or the effects of lateral heterogeneities also known as focusing or defocusing, to some extent if we know the larger-scale heterogeneities (>~1000-km wavelength). Several previous studies have introduced deterministic methods to account for these effects (*13*), providing global attenuation tomography in the upper mantle (*14*). However, the effect of lateral heterogeneities for higher-frequency waves, or scattering, is much more complicated (especially for >1 Hz) because of the larger travel distance relative to the seismic wavelength. The effect is not just the distortion of coherent waveforms, and substantial energy arrives long before or after the coherent-phase arrival times. This energy composes the incoherent parts of the seismogram (often called the coda).

Because scattering redistributes the energy of coherent seismic phases such as *P*, *S*, and surface waves into the coda, both anelasticity and scattering dissipate energy from the coherent phases. Deterministic approaches cannot be applied because we cannot resolve smaller-scale heterogeneities affecting wave propagation in these frequency ranges, although there have been deterministic studies making assumptions about the effects of heterogeneities (*13*, *15*). Alternatively, we can describe scattering as a stochastic process. Several studies have analyzed envelopes of scattered waves in this context to reveal both the anelasticity and scattering properties of the continental crust. However, many of these studies assumed that scattering properties and anelasticity are homogeneous in both the vertical and horizontal directions (*16*–*18*). In this study, we used a Monte Carlo approach to conduct accurate numerical simulations for a medium with large vertical variations (*19*, *20*), which enabled us to determine anelasticity for higher-frequency waves (~3 Hz) in both the oceanic lithosphere and asthenosphere.

Observations of higher-frequency *P* and *S* waves traveling through the oceanic LAS, often called *Po* and *So* waves, as far as a few thousand kilometers from epicenters were thought to be caused by weak intrinsic attenuation and efficient energy trapping by scattering in the lithosphere (Fig. 1A) (*21*–*26*). However, previous studies have been largely restricted to qualitative comparisons between observed and synthetic seismograms owing to limitations of the available data. The sole exception (*26*) used the distance dependence of the sum of *P* and *S* coda energies to reveal scattering properties (or the presence of laminated heterogeneities) in the lithosphere. The broadband ocean bottom seismometer (BBOBS) arrays deployed in normal oceanic regions (i.e., regions without notable tectonic activity) by the Normal Oceanic Mantle Project between 2010 and 2015 recorded abundant waveforms for the aftershocks of the 2011 Tohoku earthquake (Fig. 1B). We combined this data set with a quantitative numerical simulation approach (*20*) to independently resolve intrinsic (anelastic) and scattering attenuation. Whereas previous studies used synthetic seismograms for media with layered (*22*) or two-dimensional (2D) (*23*–*26*) random heterogeneities, we used our simulation method synthesizing seismogram envelopes for 3D randomly heterogeneous media in spherical Earth (*20*), which allowed a direct comparison between the observations and synthetics. In particular, we conducted systematic and quantitative analyses for the distance dependence of both *Po* and *So* envelope amplitudes, which are crucial to obtaining tight constraints on the anelasticity of the oceanic LAS.

Our data set covered a wide distance range (7° to 22°), which revealed the distance dependence of the envelopes in detail (Fig. 2). One of the most distinctive features of *Po* and *So* waves is that the spatial attenuation is nearly constant regardless of the wave type (*P* or *S*) or frequency (*27*). We parameterized the observed envelopes (Fig. 3A), which exhibit nearly exponential decay (Figs. 2 and 3, B and C). However, an analysis of a large number of events also revealed that the decay rate of the *Po* amplitudes at larger distances is slightly lower than that predicted by exponential decay (Figs. 2 and 3B). Regarding the relative amplitudes of *So* over *Po*, we found that the ratio is almost independent of distance (Fig. 3C). We conducted a

[1]Earthquake Research Institute, The University of Tokyo, Yayoi 1-1-1, Bunkyo-ku, Tokyo 1130032, Japan. [2]Graduate School of Science, Kobe University, 1-1, Rokkodai-cho, Nada-ku, Kobe, Hyogo 6578501, Japan. [3]Japan Agency for Marine-Earth Science and Technology, Natsushima-cho 2-15, Yokosuka-shi, Kanagawa 2370061, Japan.
*Corresponding author. Email: takeuchi@eri.u-tokyo.ac.jp

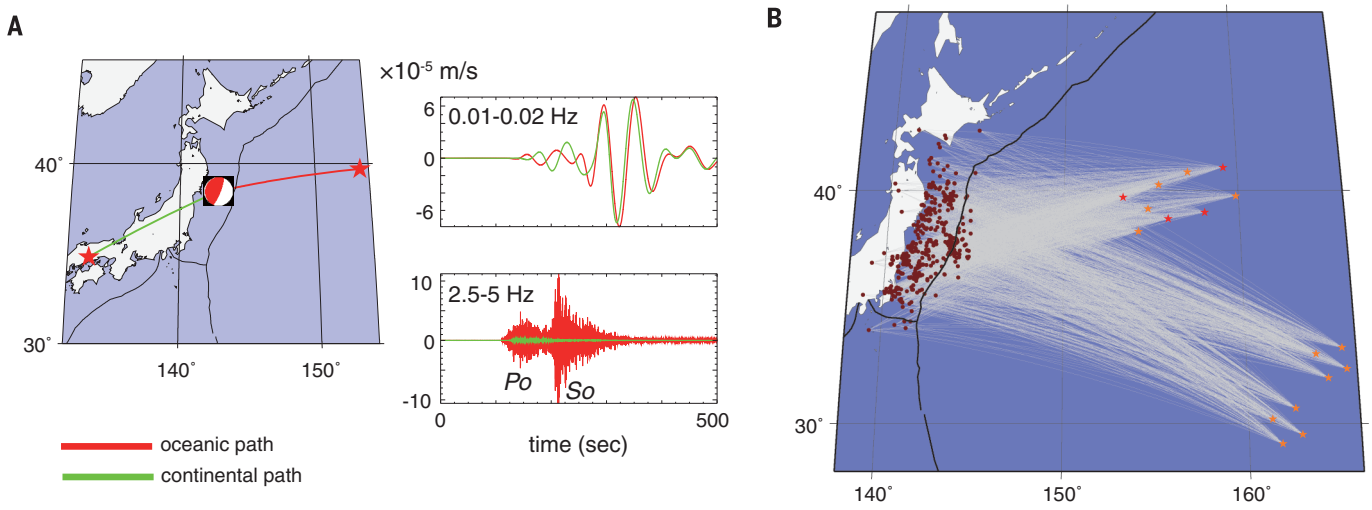

Fig. 1. Our waveform data in the northwest Pacific. (**A**) An example of an observed seismogram traveling through an oceanic path (red) and a continental path (green). The waveforms of the vertical components for the same event at almost identical distances (angular distance of 8.3°) are shown. Longer (0.01 to 0.02 Hz)– and shorter (2.5 to 5 Hz)–period components are compared. (**B**) Distribution of the events (denoted by dark red circles), stations (stars), and great circle paths (gray lines) used in our analysis. Plate boundaries (denoted by thick black lines) are overplotted for reference.

grid search for intrinsic and scattering attenuation in the oceanic lithosphere and asthenosphere to find the optimal model to explain the distance dependence of the amplitudes, A_p and A_s, as well as the peak times, t_p and t_s. Our numerical analysis indicates that the decay rate of A_p at smaller distances is primarily controlled by scattering attenuation in the lithosphere, but, at larger distances, is also controlled by intrinsic attenuation in the asthenosphere. The A_p/A_s ratio is primarily controlled by the relative importance of intrinsic and scattering attenuation in the lithosphere (see the supplementary materials for details).

Our preferred model shows strong intrinsic attenuation (Q_s = 60, where Q_s is the quality factor of the S wave, and Q^{-1} measures the strength of attenuation) in the asthenosphere, in sharp contrast with weak intrinsic attenuation (Q_s = 3200) in the lithosphere. This optimal model successfully explains most of the observed features (Figs. 2 and 3, B and C). The observed distance dependence of the *Po* amplitudes constrains the intrinsic attenuation in the asthenosphere to 30 < Q_s < 100 (Fig. 3B); further increases in Q_s cause an abrupt decrease in the decay rate of P envelopes at larger distances, whereas further decreases in Q_s lead to constant decay rates at all distances. Both of these effects are inconsistent with the observed slight decrease in decay rate at larger distances. Changing the scattering in the asthenosphere does not have a notable impact on the envelopes. We can therefore conclude that strong intrinsic attenuation in the asthenosphere is robust and is resolved independently of scattering.

By contrast, our preferred model shows weak intrinsic attenuation (Q_s = 3200) in the lithosphere. Our observation of distance independence in the ratio of *So* and *Po* amplitudes (Fig. 3C) requires this weak attenuation. To show that our method can clearly separate intrinsic and scattering attenuation, which is critical for the accurate constraint of anelasticity in the lithosphere, we compared the synthetic envelopes for cases with increased intrinsic or scattering attenuation (figs. S5, A and B). An increase in intrinsic attenuation causes a more marked decrease in *So* amplitude than in *Po* amplitude, whereas scattering attenuation has a stronger effect on *Po* amplitude. Our results show clearly that the two types of attenuation have different impacts on the envelopes. Although the discussion above depends somewhat on our assumption of the absence of bulk attenuation, the conclusions remain the same as long as the bulk attenuation is less than 20% of the *S*-wave attenuation (see the supplementary materials for details).

Previous studies that analyzed global surface waves (~100 s) (*14*), regional surface waves (17 to

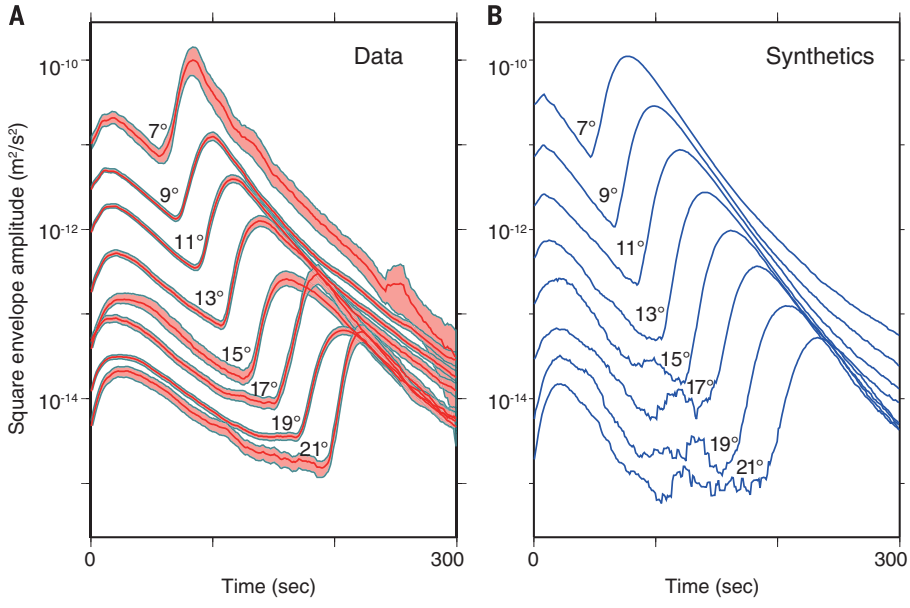

Fig. 2. Comparison of observed and synthetic envelopes. (**A**) The observed stacked envelopes for each distance bin with 1σ uncertainties estimated by the bootstrap technique and (**B**) the synthetic envelopes for our preferred model. The vertical axes are plotted on a logarithmic scale, and the horizontal axis denotes time relative to the synthetic first arrivals for the standard 1D Earth model, IASP91 (*36*). Envelopes for all distance bins are plotted on a common vertical scale.

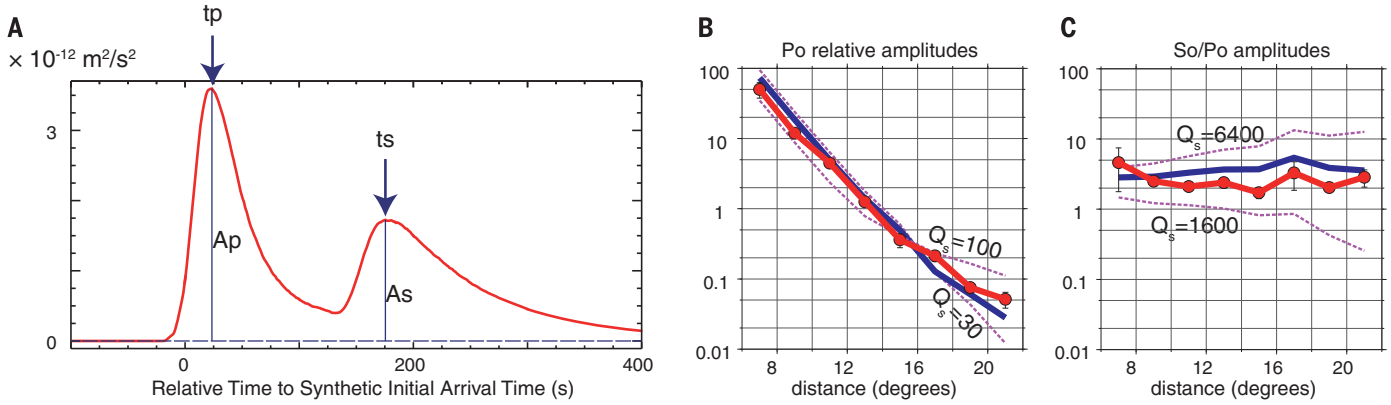

Fig. 3. Fitting of the parameterized envelopes. (**A**) Illustration of the parameters used to describe the features of square envelopes. A_p and A_s are the peak envelope amplitudes of the *Po* and *So* waves, respectively, and t_p and t_s are the peak times of the *Po* and *So* waves, respectively. (**B**) *Po* amplitudes normalized by the geometric average over all distances and (**C**) *So/Po* amplitudes. Values for the observed envelopes are shown by solid red lines, whereas those of synthetic envelopes for our preferred model and the perturbed models are shown by the solid blue lines and dashed purple lines, respectively. The tested perturbed models include those with (B) decreased intrinsic attenuation (Q_s = 60→100) and increased intrinsic attenuation (Q_s = 60→30) in the asthenosphere and (C) decreased intrinsic attenuation (Q_s = 3200→6400) and increased intrinsic attenuation (Q_s = 3200→1600) in the lithosphere. The vertical axes are plotted on a logarithmic scale.

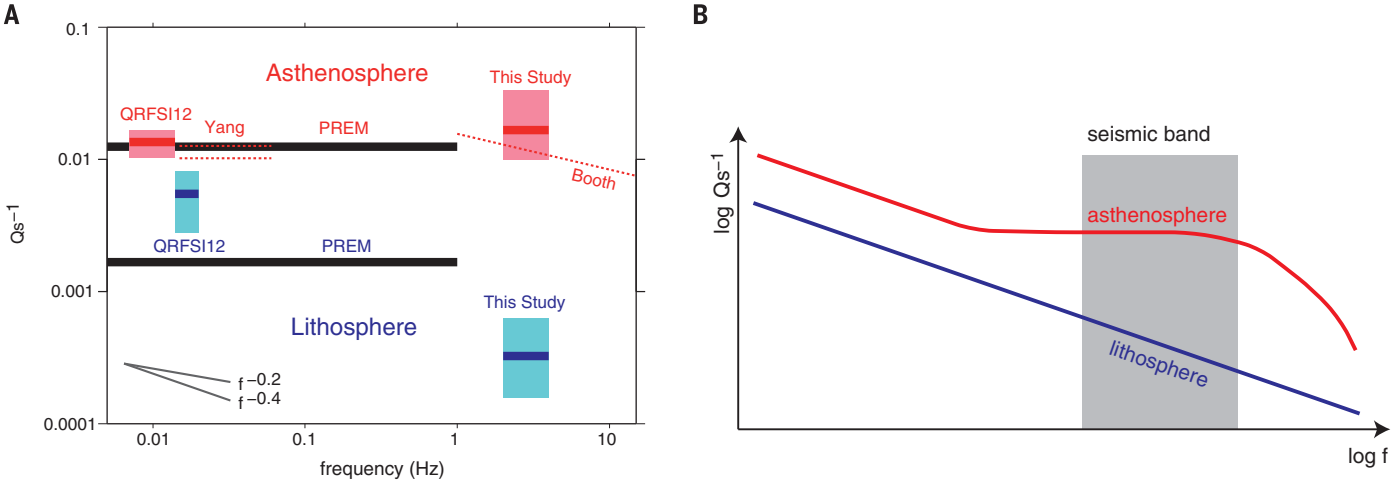

Fig. 4. Inferred anelasticity spectra. (**A**) Comparison of intrinsic *S*-wave attenuation, Q^{-1}, for the oceanic asthenosphere and lithosphere obtained by various studies as a function of the frequency range used in each analysis. We compare the PREM model (*29*), the oceanic part of the QRFSI12 model (*14*), a regional model beneath the East Pacific Rise (*28*), a regional model beneath the oldest Pacific (*15*), and the results of this study. Both axes are plotted on a logarithmic scale. The expected slopes for the $f^{-0.2}$ and $f^{-0.4}$ frequency dependencies are shown for reference. (**B**) Schematic of the suggested frequency dependence of the intrinsic attenuation in the asthenosphere (red) and lithosphere (blue). The seismic band is denoted by the shaded region.

67 s) (*28*), or regional direct *P* waves (>1 Hz) (*15*) to determine the attenuation structure of the oceanic asthenosphere found that Q_s = 50 to 100. These results are close to the PREM (Q_s = 80) (*29*) and are consistent with our results. By contrast, for the lithosphere, the results of global surface-wave analysis (~60 s) (*14*) and the PREM (Q_s = 600) (*29*) exhibit much stronger attenuation than our preferred model (Fig. 4A). This suggests that the intrinsic attenuation has a strong frequency dependence in the lithosphere, which is consistent with a power law proportional to $f^{-0.2\sim-0.4}$, where f is the frequency, but a weak frequency dependence (at least, up to 3 Hz) in the asthenosphere.

The cause of strong attenuation in the oceanic asthenosphere is still under debate and has been previously attributed to the presence of partial melt (*30*), increased water content (*31*), or reduced grain size (*32*). The frequency dependence constrained by this study provides new insight into this problem. Laboratory experiments show that, while power-law frequency dependence is widely observed (*10*, *32*), partial melting generally results in weak frequency dependence (*12*). Although similar spectrum shapes are observed even slightly below the solidus temperature in several experiments (*10*, *11*), our results (Fig. 4A) can be interpreted either way as the existence of a strong and broad absorption peak in the asthenosphere (Fig. 4B). Recent experimental studies suggested that such peaks are related to melt and are probably the consequence of melt squirt (*33*, *34*). If those experiments are assumed to be relevant to the conditions of the oceanic LAS, our results indicate the presence of partial melt in the asthenosphere. However, other experimental studies suggested that such peaks are mostly related to a solid-state mechanism rather than melt squirt (*11*), and, in that case, the existence of grain boundary softening characterizes the asthenosphere. In either case, the new constraints on the frequency dependence of the intrinsic attenuation presented here illuminate the thermochemical state of the LAS. Previous seismological studies primarily constrained the material properties and state of the oceanic LAS from correlations between *S* velocity and attenuation (*35*) for longer-period surface waves. The results of this study show that seismology has now advanced sufficiently to allow direct probes of the broadband

frequency dependence of intrinsic attenuation in the oceanic LAS. The methodology established in this study, together with further understanding of the physical mechanism of seismic attenuation, should eventually enable us to resolve the long-standing enigma of plate tectonics—i.e., which thermomechanical conditions distinguish the asthenosphere from the lithosphere.

REFERENCES AND NOTES

1. H. Kawakatsu *et al*., *Science* **324**, 499–502 (2009).
2. N. Schmerr, *Science* **335**, 1480–1483 (2012).
3. S. Naif, K. Key, S. Constable, R. L. Evans, *Nature* **495**, 356–359 (2013).
4. T. A. Stern *et al*., *Nature* **518**, 85–88 (2015).
5. W. B. Hawley, R. M. Allen, M. A. Richards, *Science* **353**, 1406–1408 (2016).
6. A. Takeo *et al*., *J. Geophys. Res.* **118**, 2878–2892 (2013).
7. A. Takeo *et al*., *J. Geophys. Res. Solid Earth* **121**, 1927–1947 (2016).
8. P.-Y. P. Lin *et al*., *Nature* **535**, 538–541 (2016).
9. H. Kawakatsu, H. Utada, *Annu. Rev. Earth Planet. Sci.* **45**, 139–167 (2017).
10. Y. Takei, F. Karasawa, H. Yamauchi, *J. Geophys. Res. Solid Earth* **119**, 5414–5443 (2014).
11. H. Yamauchi, Y. Takei, *J. Geophys. Res. Solid Earth* **121**, 7790–7820 (2016).
12. I. Jackson, U. H. Faul, J. D. Fitz Gerald, B. H. Tan, *J. Geophys. Res.* **109**, B06201 (2004).
13. B. Romanowicz, B. J. Mitchell, in *Treatise on Geophysics*, G. Schubert, Ed. (Elsevier, ed. 2, 2015), vol. 1, p. 789.
14. C. A. Dalton, G. Ekström, A. M. Dziewoński, *J. Geophys. Res.* **113**, B09303 (2008).
15. C. M. Booth, D. W. Forsyth, D. S. Weeraratne, *J. Geophys. Res. Solid Earth* **119**, 3448–3461 (2014).
16. M. Fehler, M. Hoshiba, H. Sato, K. Obara, *Geophys. J. Int.* **108**, 787–800 (1992).
17. M. Hoshiba, *J. Geophys. Res. Solid Earth* **98**, 15809–15824 (1993).
18. E. Carcolé, H. Sato, *Geophys. J. Int.* **180**, 268–290 (2010).
19. P. M. Shearer, P. S. Earle, *Geophys. J. Int.* **158**, 1103–1117 (2004).
20. N. Takeuchi, *J. Geophys. Res. Solid Earth* **121**, 3428–3444 (2016).
21. T. J. Sereno Jr., J. A. Orcutt, *J. Geophys. Res.* **92**, 3541 (1987).
22. S. Mallick, L. N. Frazer, *Geophys. J. Int.* **100**, 235–253 (1990).
23. A. Shito, D. Suetsugu, T. Furumura, H. Sugioka, A. Ito, *Geophys. Res. Lett.* **40**, 1708–1712 (2013).
24. B. L. N. Kennett, T. Furumura, *Geophys. J. Int.* **195**, 1862–1877 (2013).
25. B. L. N. Kennett, T. Furumura, Y. Zhao, *Geophys. J. Int.* **199**, 614–630 (2014).
26. A. Shito, D. Suetsugu, T. Furumura, *J. Geophys. Res. Solid Earth* **120**, 5238–5248 (2015).
27. R. Butler, C. S. McCreery, L. N. Frazer, D. A. Walker, *J. Geophys. Res.* **92**, 1383–1396 (1987).
28. Y. Yang, D. W. Forsyth, D. S. Weeraratne, *Earth Planet. Sci. Lett.* **258**, 260–268 (2007).
29. A. M. Dziewonski, D. L. Anderson, *Phys. Earth Planet. Inter.* **25**, 297–356 (1981).
30. D. L. Anderson, C. G. Sammis, *Phys. Earth Planet. Inter.* **3**, 41–50 (1970).
31. G. Hirth, D. L. Kohlstedt, *Earth Planet. Sci. Lett.* **144**, 93–108 (1996).
32. I. Jackson, U. H. Faul, *Phys. Earth Planet. Inter.* **183**, 151–163 (2010).
33. U. Faul, I. Jackson, *Annu. Rev. Earth Planet. Sci.* **43**, 541–569 (2015).
34. I. Jackson, in *Treatise in Geophysics*, G. Schubert, Ed. (Elsevier, ed. 2, 2015), vol. 2, p. 539.
35. Y. Takei, *Annu. Rev. Earth Planet. Sci.* **45**, 447–470 (2017).
36. B. L. N. Kennett, E. R. Engdahl, *Geophys. J. Int.* **105**, 429–465 (1991).

ACKNOWLEDGMENTS

This research was partially supported by KAKENHI grants JP22000003, JP25400439, and JP15H05832 from the Japan Society for the Promotion of Science. We thank Y. Takei for useful discussions. All of the waveform data used in this study are available at http://ohpdmc.eri.u-tokyo.ac.jp/.

SUPPLEMENTARY MATERIALS

www.sciencemag.org/content/358/6370/1593/suppl/DC1
Materials and Methods
Supplementary Text
Figs. S1 to S11
Tables S1 and S2
References (*37*–*44*)

11 July 2017; accepted 6 November 2017
10.1126/science.aao3508

Science

Determination of intrinsic attenuation in the oceanic lithosphere-asthenosphere system

Nozomu Takeuchi, Hitoshi Kawakatsu, Hajime Shiobara, Takehi Isse, Hiroko Sugioka, Aki Ito and Hisashi Utada

Science **358** (6370), 1593-1596.
DOI: 10.1126/science.aao3508

Determining damping of our plates

For plate tectonics to operate, a weaker layer called the asthenosphere must underlie the rigid lithospheric plates. Quantifying the difference in strength comes down to how much each layer attenuates energy. Takeuchi *et al.* exploited an ocean-bottom seismic network and seismic energy from the 2011 Japanese Tohoku-oki earthquake to quantify the attenuation in each layer (see the Perspective by Dalton). The attenuation of energy in the asthenosphere lined up with previous estimates, but the lithospheric attenuation was roughly one-fifth as strong as that predicted by some previous models.

Science, this issue p. 1593; see also p. 1536

Science (print ISSN 0036-8075; online ISSN 1095-9203) is published by the American Association for the Advancement of Science, 1200 New York Avenue NW, Washington, DC 20005.